Eur. Phys. J. C 23, 591–596 (2002)
Digital Object Identifier (DOI) 10.1007/s100520200899

THE EUROPEAN PHYSICAL JOURNAL C

Quark number susceptibility in hard thermal loop approximation

P. Chakraborty[1], M.G. Mustafa[1], M.H. Thoma[2]

[1] Theory Group, Saha Institute of Nuclear Physics, 1/AF Bidhan Nagar, Kolkata 700 064, India
[2] Max-Planck-Institut für extraterrestrische Physik, Giessenbachstraße, 85748 Garching, Germany

Received: 7 December 2001 /
Published online: 15 March 2002 –

Abstract. We calculate the quark number susceptibility in the deconfined phase of QCD using the hard thermal loop (HTL) approximation for the quark propagator and quark–meson vertices. This improved perturbation theory takes into account important medium effects such as thermal quark masses and Landau damping in the quark–gluon plasma. We explicitly show that the Landau damping part in the quark propagator for space-like quark momenta does not contribute to the quark number susceptibility due to the quark number conservation. We find that the quark number susceptibility only due to the collective quark modes deviates from the free one around the critical temperature but approaches free results in the infinite temperature limit. The results are in conformity with recent lattice calculations.

In recent years substantial experimental and theoretical efforts have been undertaken to investigate the versatile physics issues involved in ultra-relativistic heavy-ion collisions, i.e., collisions of atomic nuclei in which the center-of-mass energy per nucleon is much larger than the nucleon rest mass. The principal goal of this initiative is to explore the phase structure of the underlying theory of strong interactions – quantum chromodynamics (QCD) – by creating in the laboratory a new state of matter, the so-called quark–gluon plasma (QGP). This new state of matter is predicted to exist under extreme conditions like at high temperatures and/or densities, when a phase transition takes place from a hadronic to a deconfined state of quarks and gluons [1]. Such information has essentially been confirmed by numerical lattice QCD calculations [2] at finite temperature, which show a rapid increase in energy density and entropy density as a function of temperature. Numerical solutions of QCD also suggest that the critical temperature is about 170 MeV [3] and provide information on the equation of state [4].

The various measurements taken at CERN SPS within the Lead Beam Programme do lead to strong "circumstantial evidence" for the formation of the QGP [5,6]. The evidence is circumstantial as any direct formation of the QGP cannot be identified. Only by some noble indirect diagnostic probes like the suppression of the J/Ψ particle, the enhanced production of strange particles, especially strange antibaryons, excess production of photons and dileptons, the formation of disoriented chiral condensates, etc. this discovery can be achieved. A great amount of theoretical study has also been devoted over the last two decades in favour of these well accepted probes of a deconfinement (QGP) phase.

Recently screening and fluctuation of conserved quantities have been considered as important and relevant probes of the QGP formation in heavy-ion collisions [7–10]. In the confined/chirally broken phase charges are associated with the hadrons in integer units whereas in the deconfined/chirally restored phase they are associated with the quarks in fractional units which could lead to charge fluctuations which are different in the two phases [7,10]. The fluctuations can generally be related to the associated susceptibilities [7,11]. The quark number susceptibility is associated with the number fluctuation which measures the response of the number density with infinitesimal change of the quark chemical potential. Hence the quark number susceptibility can be related to charge fluctuations [10] and is therefore of direct experimental relevance. The quark number susceptibility has been investigated in lattice QCD simulations [12] which showed that it is zero at low temperature and increases suddenly to non-zero values across the deconfinement phase transition. At high temperature QCD it has been analysed [13] and one has shown non-perturbative temperature effects at next-to-leading order. Recently, this has been discussed [14] in connection with the role of the fluctuations during the dense stages of the collision with the aim to exploit the electromagnetic probes with the hadronic probes. A very recent lattice simulation [15] has verified a new relation between susceptibilities and screening masses and explains that the non-perturbative phenomena are closely connected with deviations from the weak coupling limit or bare perturbation theory, indicating the need to resum the weak coupling series. The purpose of the present calculation is to investigate the quark number susceptibility within the HTL resummed perturbation theory which incorporates non-perturbative effects such as effective masses of the collective quark modes (quark and plasmino modes in the medium originating from the poles of the HTL propagator) and Landau damping for space-like quark momenta, reflecting the physical picture of the QGP as a gas of quasiparticles. As we will see below, the quark number susceptibility obtained in HTL approximation is in agreement with recent lattice [15] observations.

1 Fluctuation and susceptibility

Let $\mathcal{O}_\alpha$ be a Heisenberg operator. In a static and uniform external field $\mathcal{F}_\alpha$, the (induced) expectation value of the operator $\mathcal{O}_\alpha(0,\boldsymbol{x})$ is written [11] as

$$\phi_\alpha \equiv \langle \mathcal{O}_\alpha(0,\boldsymbol{x})\rangle_F = \frac{\mathrm{Tr}\left[\mathcal{O}_\alpha(0,\boldsymbol{x})\,\mathrm{e}^{-\beta(\mathcal{H}+\mathcal{H}_{\mathrm{ex}})}\right]}{\mathrm{Tr}\left[\mathrm{e}^{-\beta(\mathcal{H}+\mathcal{H}_{\mathrm{ex}})}\right]} = \frac{1}{V}\int \mathrm{d}^3x\,\langle \mathcal{O}_\alpha(0,\boldsymbol{x})\rangle\,, \quad (1)$$

where translational invariance is assumed and $\mathcal{H}_{\mathrm{ex}}$ is given by

$$\mathcal{H}_{\mathrm{ex}} = -\sum_\alpha \int \mathrm{d}^3x\,\mathcal{O}_\alpha(0,\boldsymbol{x})\,\mathcal{F}_\alpha\,. \quad (2)$$

The (static) susceptibility $\chi_{\alpha\beta}$ is defined as

$$\chi_{\alpha\sigma}(T) = \left.\frac{\partial\phi_\alpha}{\partial\mathcal{F}_\sigma}\right|_{\mathcal{F}=0} = \beta\int \mathrm{d}^3x\,\langle \mathcal{O}_\alpha(0,\boldsymbol{x})\,\mathcal{O}_\sigma(0,\boldsymbol{0})\rangle\,, \quad (3)$$

assuming no broken symmetry

$$\langle \mathcal{O}_\alpha(0,\boldsymbol{x})\rangle = \langle \mathcal{O}_\sigma(0,\boldsymbol{0})\rangle = 0.$$

$\langle \mathcal{O}_\alpha(0,\boldsymbol{x})\mathcal{O}_\sigma(0,\boldsymbol{0})\rangle$ is the two point correlation function with operators evaluated at equal times.

2 Quark number susceptibility

The quark number susceptibility is the measure of the response of the quark number density with infinitesimal changes in the quark chemical potential, $\mu_q+\delta\mu_q$. In such a situation the external field, $\mathcal{F}_\alpha$, in (2) can be identified as the change in quark chemical potential μ_q and the operator $\mathcal{O}_\alpha$: $j_0=\overline{q}\gamma_0 q$, where $j_\mu(t,\boldsymbol{x})=\overline{q}\gamma_\mu q$ is the vector meson current. Then the quark number susceptibility for a given quark flavour follows from (3);

$$\chi_q(T) = \left.\frac{\partial\rho_q}{\partial\mu_q}\right|_{\mu_q=0} = \beta\int \mathrm{d}^3x\,\langle j_0(0,\boldsymbol{x})j_0(0,\boldsymbol{0})\rangle = \beta\int \mathrm{d}^3x S_{00}(0,\boldsymbol{x}), \quad (4)$$

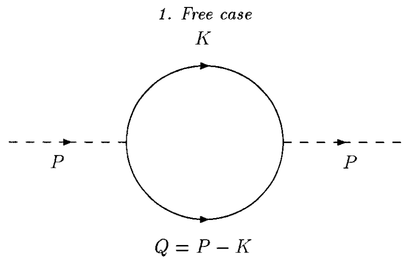

Fig. 1. The self-energy diagram for free quarks

where $S_{00}(0,\boldsymbol{x})$ is the time–time component of the vector meson correlator $S_{\mu\nu}(t,\boldsymbol{x}) = \langle j_\mu(t,\boldsymbol{x})j_\nu(0,\boldsymbol{0})\rangle$ and the number density can be written as

$$\rho_q = \frac{1}{V}\frac{\mathrm{Tr}\left[\mathcal{N}_q\mathrm{e}^{-\beta(\mathcal{H}-\mu_q\mathcal{N}_q)}\right]}{\mathrm{Tr}\left[\mathrm{e}^{-\beta(\mathcal{H}-\mu_q\mathcal{N}_q)}\right]} = \frac{\langle\mathcal{N}_q\rangle}{V} = -\frac{1}{V}\frac{\partial\Omega}{\partial\mu_q}, \quad (5)$$

with the quark number operator, $\mathcal{N}_q = \int j_0(t,\boldsymbol{x})\mathrm{d}^3x$, and $\Omega = -T\ln Z$ is the thermodynamic potential and Z the partition function of a quark–antiquark gas.

Taking the Fourier transform of $S_{00}(0,\boldsymbol{x})$, it can be shown that [11]

$$\chi_q(T) = \lim_{p\to 0}\beta\int_{-\infty}^{+\infty}\frac{\mathrm{d}\omega}{2\pi}S_{00}(\omega,p)\,. \quad (6)$$

Using the fluctuation-dissipation theorem [16], it can further be shown that [11]

$$\chi_q(T) = \beta\int_{-\infty}^{+\infty}\frac{\mathrm{d}\omega}{2\pi}\frac{-2}{1-\mathrm{e}^{-\beta\omega}}\,\mathrm{Im}\,\Pi_{00}(\omega,0)\,, \quad (7)$$

where

$$\Pi_{\mu\nu}(\omega,\boldsymbol{p}) = \mathrm{FT}\left(-\mathrm{i}\theta(t)\left\langle[j_\mu(t,\boldsymbol{x}),j_\nu(0,\boldsymbol{0})]_-\right\rangle\right),$$

and FT stands for Fourier transformation.

2.1 Free case

To lowest order in perturbation theory one has to evaluate the time–time component of the self-energy diagram shown in Fig. 1, where the internal quark lines represent a bare quark propagator $S_f(L)$ which can be expressed in the helicity representation for the massless case by ($L=(l_0,\boldsymbol{l})$, $l=|\boldsymbol{l}\,|$) [17]

$$S_f(l_0,l) = \frac{\gamma^0-\widehat{l}.\boldsymbol{\gamma}}{2d_+(L)} + \frac{\gamma^0+\widehat{l}.\boldsymbol{\gamma}}{2d_-(L)}, \quad (8)$$

with

$$d_\pm(l_0,l) = -l_0 \pm l. \quad (9)$$

The corresponding spectral function is given by

$$\rho_\pm^f(l_0,l) = \delta(l_0\mp l)\,. \quad (10)$$

Now the time–time component of the vector meson self-energy in Fig. 1 can be written as

$$\Pi^{00}(P) = N_f N_c T \sum_{k_0} \int \frac{\mathrm{d}^3k}{(2\pi)^3} \mathrm{Tr}\left[S_f(K)\gamma^0 S_f(Q)\gamma^0\right], \tag{11}$$

where $Q = P - K$, and N_f and N_c are, respectively, the number of quark flavours and colours.

Substituting the propagator (8) in (11), performing the trace, and following the summation relation of [17], we extract the imaginary part as

$$\begin{aligned}\mathrm{Im}\,\Pi^{00}(\omega, \boldsymbol{p}=0) &= \\ 4N_f N_c \pi \left(1 - \mathrm{e}^{\beta\omega}\right) &\int \frac{\mathrm{d}^3k}{(2\pi)^3} \int \mathrm{d}x \int \mathrm{d}x' \delta(\omega - x - x') \\ &\times n_{\mathrm{F}}(x)\, n_{\mathrm{F}}(x')\, \rho_+^f(x,k)\, \rho_-^f(x',k),\end{aligned} \tag{12}$$

where x and x' are the energies of the internal quarks and n_{F} is the Fermi distribution function. Using (10) in (12), we get

$$\begin{aligned}\mathrm{Im}\Pi^{00}(\omega, \boldsymbol{p}=0) &= \\ 4N_c N_f \pi \left(1 - \mathrm{e}^{\beta\omega}\right)\delta(\omega) &\int \frac{\mathrm{d}^3k}{(2\pi)^3} n_{\mathrm{F}}(k)\left(1 - n_{\mathrm{F}}(k)\right).\end{aligned} \tag{13}$$

Inserting (13) in (7), we obtain the quark number susceptibility in lowest order perturbation theory [7,11]

$$\chi_q^f(T) = 4N_f N_c \beta \int \frac{\mathrm{d}^3k}{(2\pi)^3} \frac{\mathrm{e}^{\beta k}}{\left(1 + \mathrm{e}^{\beta k}\right)^2}. \tag{14}$$

Alternatively, considering the lowest order thermodynamic potential of a quark–antiquark gas [18,19]

$$\begin{aligned}\Omega = -2N_f N_c T \int \frac{\mathrm{d}^3k}{(2\pi)^3} &\left[\beta E_k + \ln\left(1 + \mathrm{e}^{-\beta(E_k - \mu_q)}\right)\right. \\ &\left. + \ln\left(1 + \mathrm{e}^{-\beta(E_k + \mu_q)}\right)\right],\end{aligned} \tag{15}$$

one could arrive at the same expression using (4) and (5).

Due to the quark number conservation $\mathrm{Im}\Pi(\omega, 0)$, as obtained in (13), is proportional to $\delta(\omega)$. This leads to a general relation between the quark number susceptibility and the time–time component of the polarisation tensor in the vector channel,

$$\begin{aligned}\chi_q^f(T) = -4N_f N_c \int \frac{\mathrm{d}^3k}{(2\pi)^3} \frac{\mathrm{d}n_{\mathrm{F}}}{\mathrm{d}k} &\equiv -\mathrm{Re}\Pi_{00}(0,0) \\ &\equiv (\mu_D^f)^2,\end{aligned} \tag{16}$$

which provides a connection [11,14,18–20] to the electric screening mass, μ_D^f. This relation is only valid in lowest order in perturbation theory.

2.2 HTL case

Now we turn to the estimate of the quark number susceptibility beyond the free quark approximation by invoking the in-medium properties of quarks in a QGP. In the weak coupling limit ($g \ll 1$), a consistent method is to use the HTL resummed quark propagators and HTL quark–meson vertex if the quark momentum is soft ($\sim gT$). Using this improved perturbation theory at least to some extent nonperturbative features of the QGP such as effective quark masses and Landau damping are incorporated through the effective quantities like quark propagators and the quark–meson vertex.

Let us, however, note that we do not aim at a complete leading order perturbative calculation. Rather we want to study the influence of medium effects incorporated in the HTL resummed quark propagator. Hence, we will use this propagator for the entire momentum range instead of consistently distinguishing between soft and hard momenta [21]. Anyway, since this distinction is only possible in the weak coupling limit, $g \ll 1$, it cannot be used in our case, in which we want to compare our results to QCD lattice calculations. The approach considered here is in the same spirit as the one for calculating meson correlators in the QGP [22]. It should be noticed that our results are gauge independent due to the gauge invariance of the HTL quark propagator.

The HTL resummed quark propagator, $S^\star(L)$, can be obtained [17] from (8) by replacing $d_\pm(L)$:

$$D_\pm(l_0, l) = -l_0 \pm l + \frac{m_q^2}{l}\left[Q_0\left(\frac{l_0}{l}\right) \mp Q_1\left(\frac{l_0}{l}\right)\right], \tag{17}$$

where the thermal quark mass is given by $m_q = g(T)T/(6^{1/2})$, and $Q_n(y)$ is the Legendre function of second kind. The HTL vertex can be obtained [23] as

$$\Gamma^\mu(P_1, P_2) = \gamma^\mu + m_q^2 G^{\mu\nu}\gamma_\nu, \tag{18}$$

with

$$\begin{aligned}G^{\mu\nu}(P_1, P_2) &= \int \frac{\mathrm{d}\Omega}{4\pi} \frac{R^\mu R^\nu}{(R\cdot P_1)(R\cdot P_2)} \\ &= G^{\mu\nu}(-P_1, -P_2),\end{aligned} \tag{19}$$

where $R \equiv (-1, \boldsymbol{r})$ is a light-like four vector, $R^2 = 0$. The effective propagator and vertex are related via the Ward identity.

The HTL spectral function reads [17]

$$\begin{aligned}\rho_\pm(l_0, l) = &\frac{l_0^2 - l^2}{2m_q^2}\left[\delta(l_0 - \omega_\pm) + \delta(l_0 + \omega_\mp)\right] \\ &+ \beta_\pm(l_0, l)\Theta(l^2 - l_0^2),\end{aligned} \tag{20}$$

with

$$\begin{aligned}\beta_\pm(l_0, l) = &-\frac{m_q^2}{2}(\pm l_0 - l) \\ &\times\left\{\left[l(-l_0 \pm l) + m_q^2\left(\pm 1 - \frac{\pm l_0 - l}{2l}\ln\frac{l + l_0}{l - l_0}\right)\right]^2\right. \\ &\left. + \left[\frac{\pi}{2} m_q^2 \frac{\pm l_0 - l}{l}\right]^2\right\}^{-1}.\end{aligned} \tag{21}$$

Here the zeros $\omega_\pm(l)$ of $D_\pm(L)$ describe the two branches of the dispersion relation of collective quark modes in a

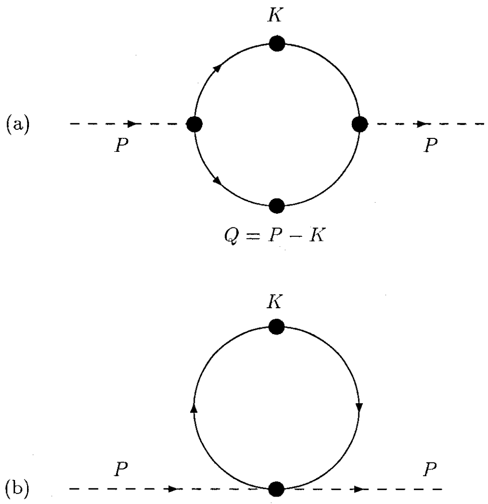

Fig. 2a,b. The self-energy **a** and tadpole **b** diagrams for quarks in the HTL approximation

thermal medium [17]. Furthermore the HTL resummed quark propagator acquires a cut contribution below the light cone ($l_0^2 < l^2$) as the quark self-energy has a non-vanishing imaginary part, which can be related to Landau damping for space-like quark momenta resulting from interactions of valence quarks with gluons in the thermal medium. In addition, an explicit temperature dependence only enters through $m_q(T)$ as well as through the strong coupling constant, $g^2(T) = 4\pi\alpha_s(T)$ with

$$\alpha_s(T) = \frac{12\pi}{(33 - 2N_f)\ln(Q^2/\Lambda_0^2)}, \tag{22}$$

where $\Lambda_0 = 200$–$300\,\mathrm{MeV}$. For the momentum scale Q we take the energy of the lowest Matsubara mode $Q = 2\pi T$ [24]. For checking the sensitivity of the susceptibility to uncertainties in the coupling constant we will use also $Q = 4\pi T$. It should also be noted that the HTL resummed propagator is chirally symmetric in spite of the appearance of an effective quark mass [17].

Now we need to calculate the imaginary part of the time–time component of the self-energy diagrams given in Fig. 2, in which blobs represent the effective quantities. The tadpole diagram in Fig. 2b is essential to satisfy the transversality condition, $P_\mu \Pi^{\mu\nu}(P) = 0$. As will be seen below this has a very important effect on the quark number susceptibility by partially compensating the cut contribution in diagram Fig. 2a.

Now the time–time component of the self-energy in diagram Fig. 2a can be written as

$$\begin{aligned}\Pi_1^{00}(P) &= N_f N_c T \\ &\times \sum_{k_0} \int \frac{\mathrm{d}^3k}{(2\pi)^3} \mathrm{Tr}\left[S^\star(K)\,\Gamma^0(K-P,-K;P)\right. \\ &\times \left. S^\star(Q)\,\Gamma^0(P-K,K;-P)\right]. \end{aligned} \tag{23}$$

The time component of the HTL vertex can be obtained by carrying out the angular integration in (18) for $\boldsymbol{p} = 0$:

$$\Gamma^0(K-P,K;P) = \left(1 - \frac{m_q^2}{p_0 k}\delta Q_0\right)\gamma^0 + \frac{m_q^2}{p_0 k}\delta Q_1 \widehat{k}.\boldsymbol{\gamma}, \tag{24}$$

where

$$\delta Q_n = Q_n\left(\frac{k_0}{k}\right) - Q_n\left(\frac{k_0 - p_0}{k}\right). \tag{25}$$

Alternatively, $\Gamma^0(P_1, P_2)$ can also be obtained from the Ward identity $P_\mu \Gamma^\mu(P_1, P_2; P) = S^{\star -1}(P_1) - S^{\star -1}(P_2)$.

Now performing the traces in (23), we get

$$\begin{aligned}\Pi_1^{00}(p_0, \boldsymbol{p}=0) &= 2N_f N_c T \\ &\times \sum_{k_0}\int \frac{\mathrm{d}^3k}{(2\pi)^3}\left[\frac{(a+b)^2}{D_+(K)\,D_-(Q)} + \frac{(a-b)^2}{D_-(K)\,D_+(Q)}\right],\end{aligned} \tag{26}$$

where

$$a = \left(1 - \frac{m_q^2}{p_0 k}\delta Q_0\right), \quad b = \frac{m_q^2}{p_0 k}\delta Q_1,$$

$$\begin{aligned} a \pm b = 1 - \frac{m_q^2}{p_0 k}&\left\{Q_0\left(\frac{k_0}{k}\right)\left(1 \mp \frac{k_0}{k}\right)\right. \\ &\left. + Q_0\left(\frac{q_0}{k}\right)\left(1 \pm \frac{q_0}{k}\right)\right\}, \end{aligned} \tag{27}$$

where $q_0 = p_0 - k_0$ and $Q_n(-y) = (-1)^{n+1} Q_n(y)$ has been used in (27). Following the summation formula of [17] the imaginary part of (26) then can be written as

$$\begin{aligned}\mathrm{Im}\Pi_1^{00}(\omega, \boldsymbol{p}=0) &= N_f N_c \pi\left(1 - \mathrm{e}^{\beta\omega}\right) \\ &\times \int \frac{\mathrm{d}^3k}{(2\pi)^3}\int \mathrm{d}x \int \mathrm{d}x'\,\delta(\omega - x - x')\,n_{\mathrm{F}}(x)\,n_{\mathrm{F}}(x') \\ &\times \left[4\left(1 - \frac{x+x'}{\omega}\right)^2 \rho_+(x,k)\,\rho_-(x',k)\right. \\ &- 4\frac{m_q^2}{\omega^2 k}\Theta\left(k^2 - x^2\right) \\ &\times \left.\left\{\frac{1}{2}\left(1 - \frac{x}{k}\right)\rho_-(x',k) + \frac{1}{2}\left(1 + \frac{x}{k}\right)\rho_+(x',k)\right\}\right]. \end{aligned} \tag{28}$$

The contribution of the time–time component of the tadpole diagram in Fig. 2b can be written as

$$\begin{aligned}\Pi_2^{00}(P) &= N_f N_c T \sum_{k_0}\int \frac{\mathrm{d}^3k}{(2\pi)^3} \\ &\times \mathrm{Tr}\left[S^\star(K)\,\Gamma^{00}(-K,K;-P,P)\right], \end{aligned} \tag{29}$$

where the effective HTL four point function can be obtained from the relation

$$\begin{aligned}P_\mu \Gamma^{\mu\nu}(-K,K;-P,P) &= \Gamma^\nu(K-P,-K;P) \\ &- \Gamma^\nu(-K-P,K;P). \end{aligned} \tag{30}$$

At $\boldsymbol{p} = 0$ the four point function is obtained as

$$\begin{aligned}&\Gamma^{00}(-K,K;-P,P) \\ &= -\frac{m_q^2}{p_0^2 k}\left(\delta Q_0 + \delta Q_0'\right)\gamma^0 + \frac{m_q^2}{p_0^2 k}\left(\delta Q_1 + \delta Q_1'\right)\widehat{k}\cdot\boldsymbol{\gamma},\end{aligned} \tag{31}$$

with

$$\delta Q_n' = Q_n\left(\frac{k_0}{k}\right) - Q_n\left(\frac{k_0+p_0}{k}\right). \qquad (32)$$

Proceeding exactly the same way as before, we get the imaginary part of the tadpole:

$$\begin{aligned}\mathrm{Im}\Pi_2^{00}(\omega, \boldsymbol{p}=0) &= N_f N_c \pi \left(1 - \mathrm{e}^{\beta\omega}\right)\\ &\times \int \frac{\mathrm{d}^3 k}{(2\pi)^3} \int \mathrm{d}x \int \mathrm{d}x' \delta\left(\omega - x - x'\right) n_{\mathrm{F}}(x)\, n_{\mathrm{F}}(x')\\ &\times 4\frac{m_q^2}{\omega^2 k}\Theta\left(k^2 - x^2\right) \qquad (33)\\ &\times \left[\frac{1}{2}\left(1-\frac{x}{k}\right)\rho_-(x',k) + \frac{1}{2}\left(1+\frac{x}{k}\right)\rho_+(x',k)\right].\end{aligned}$$

It can be seen that the tadpole contribution compensates the second term of (28) and the total contribution becomes

$$\begin{aligned}\mathrm{Im}\,\Pi^{00}(\omega, \boldsymbol{p}=0) &= 4N_f N_c \pi \left(1 - \mathrm{e}^{\beta\omega}\right)\\ &\times \int \frac{\mathrm{d}^3 k}{(2\pi)^3} \int \mathrm{d}x \int \mathrm{d}x' \delta\left(\omega - x - x'\right) n_{\mathrm{F}}(x)\, n_{\mathrm{F}}(x')\\ &\times \left(1 - \frac{x+x'}{\omega}\right)^2 \rho_+(x,k)\,\rho_-(x',k). \qquad (34)\end{aligned}$$

Now combining (20), (34) and (7), the quark number susceptibility in HTL approximation is obtained as

$$\begin{aligned}\chi_q^h(T) &= 4N_f N_c \beta\\ &\times \int \frac{\mathrm{d}^3 k}{(2\pi)^3}\left[\frac{\left(\omega_+^2(k) - k^2\right)^2}{4m_q^4} n_{\mathrm{F}}(\omega_+)\left(1 - n_{\mathrm{F}}(\omega_+)\right)\right.\\ &\left. + \frac{\left(\omega_-^2(k) - k^2\right)^2}{4m_q^4} n_{\mathrm{F}}(\omega_-)\left(1 - n_{\mathrm{F}}(\omega_-)\right)\right]. \qquad (35)\end{aligned}$$

Since the quark number susceptibility is constructed from two quark propagators, in general they should receive pole–pole, pole–cut and cut–cut contributions [17]. However, according to (35) it has only pole–pole contributions from the two collective quark modes (quark and plasmino modes in the medium). The cut contributions (pole–cut and cut–cut) due to space-like quark momenta (Landau damping) do not contribute because of the number conservation in the system. In the high temperature limit, the second term due to the plasmino mode decouples from the medium whereas the first term reduces to the free susceptibility given in (16).

We now discuss our results for the quark number susceptibility. In Fig. 3 we present the temperature dependence of the quark number susceptibility $\chi_q(T)$ in units of $N_f T^2$, the free field theory susceptibility. We have used the temperature dependence of the strong coupling constant as given in (22) for two different ratios of T_c to Λ_0 and two different values for Q. The choice $T_c/\Lambda_0 = 0.49$ [25] has been used in the lattice calculations of [15]. We observe that the quark number susceptibility does not depend strongly on the choice of the coupling constant. (For

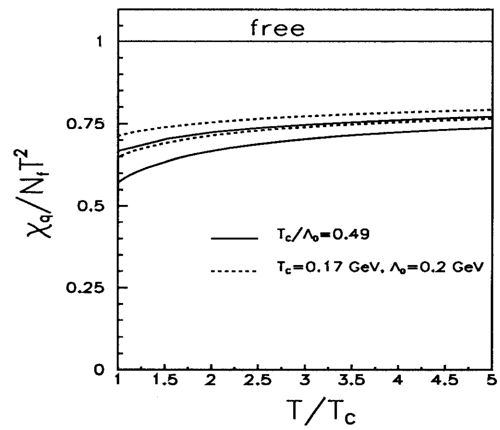

Fig. 3. $\chi_q(T)/N_f T^2$ as a function of T/T_c in the HTL approximation. N_f is the number of quark flavours and T_c is the critical temperature for the deconfined phase transition. For the solid curves (22) with $T_c/\Lambda_0 = 0.49$ [25] and for the dashed curves $\Lambda_0 = 200\,\mathrm{MeV}$ and $T_c = 170\,\mathrm{MeV}$ have been used. The lower curves correspond to $Q = 2\pi T$ and the upper ones to $Q = 4\pi T$

$T_c = 170\,\mathrm{MeV}$ and $\Lambda_0 = 300\,\mathrm{MeV}$ the susceptibility decreases by about 5% compared to the dashed curves.) The susceptibility increases with the increase of temperature. It is interesting to note that the result lies significantly below the free result even at $T = 5T_c$ and the deviation is 25–40%. This deviation agrees with the recent lattice observation [15] along with a slow approach to the free quark susceptibility. This result is reminiscent of the fact that the quark number susceptibility in HTL approximation contains non-perturbative information about the QGP phase at high temperature. In the infinite temperature limit, the HTL result exactly reproduces the free quark susceptibility. This can clearly be seen in Fig. 4 below.

In Fig. 4 we display the quark number susceptibility in units of $N_f T^2$ as function of m_q/T using (22) with $\Lambda_0 = 300\,\mathrm{MeV}$ and $Q = 2\pi T$. As expected for small thermal quark masses, the HTL susceptibility begins with the free field theory result, $N_f T^2$, with a flat tangent at $m_q = 0$ and a quadratic dependence on m_q. With the increase of the mass the susceptibility starts decreasing monotonically. For low values of the thermal quark mass, the susceptibility is large due to the fact that it is relatively easy to create an additional quark or antiquark. On the other hand, if quarks acquire thermal masses in the medium, the susceptibility decreases, which could qualitatively be understood as an effect of the Boltzmann factor.

3 Conclusion

We have calculated the quark number susceptibility in the HTL approximation which incorporates in-medium effects of the QGP phase such as quark masses and Landau damping through the HTL resummed propagators and the HTL quark–meson vertex in the vector meson channel. We have discussed the influence of the various non-

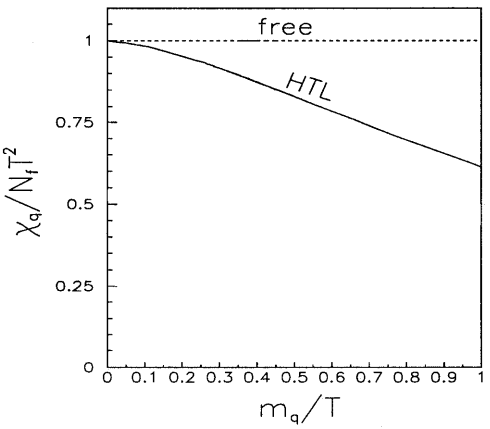

Fig. 4. $\chi_q(T)/N_fT^2$ as a function of m_q/T for free quarks (dashed line) and in the HTL approximation (solid line). m_q is the thermal quark mass

perturbative effects on the quark number susceptibility in the deconfined phase. The Landau damping contribution due to space-like quark momenta drops out because of the quark number conservation in the system. Technically this occurs partly due to a cancellation of the two diagrams in Fig. 2 containing HTL resummed quark–meson vertices, and partly due to kinematical reasons in (34).

We find that the quark number susceptibility is significantly smaller than the free susceptibility for moderately high temperatures. Our results are in good agreement with recent lattice calculations. Besides the on-set of confinement and chiral symmetry breaking close to T_c, HTL effects may explain the lattice results similar as in the case of the free energy [26] but in contrast to the meson correlation functions [22]. Since the quark number susceptibility is related to charge fluctuations, it could be an interesting observable in heavy-ion collisions.

Acknowledgements. We would like to thank S. Gupta and A. Rebhan for helpful comments. P.C. is thankful to R. Pisarski for useful communication.

References

1. B. Müller, The Physics of the Quark-Gluon Plasma, Lecture Notes in Physics 225 (Springer, Berlin, 1985); J.W. Harris, B. Müller, Annu. Rev. Nucl. Part. Sci. **46**, 71 (1996); Quark-Gluon Plasma 1 and 2 edited by R.C. Hwa (World Scientific, Singapore 1990 and 1995); C.Y. Wong, Introduction to high energy heavy ion collisions (World Scientific, Singapore 1994)
2. H. Satz, Ann. Rev. Nucl. Part. Sci. **35**, 245 (1985); F. Karsch, E. Laermann, Rept. Prog. Physics **56**, 1347 (1993)
3. F. Karsch, Lattice'99, Proceedings of the XVIIth International Symposium on Lattice Field Theory, Nucl. Phys. B (Proc. Suppl.) **83–84**, 14c (2000); F. Karsch et al., Nucl. Phys. B **605**, 579 (2001); S. Gupta, Phys. Rev. D **64**, 034507 (2001); A. Ali Khan et al., Phys. Rev. D **63**, 034502 (2001)
4. F. Karsch, Phys. Lett. B **478**, 447 (2000); A. Ali Khan et al., Phys. Rev. D **64**, 074510 (2001)
5. Proceedings of the 14th International Conference on Ultra-Relativistic Nucleus–Nucleus Collisions "Quark Matter'99", Nucl. Phys. A **661**, (2000)
6. Proceedings of the 15th International Conference on Ultra-Relativistic Nucleus–Nucleus Collisions "Quark Matter'01" (to appear in Nucl. Phys. A)
7. L. McLerran, Phys. Rev. D **36**, 3291 (1987)
8. M. Roland et al. (NA49 Collaboration), Nucl. Phys. A **638**, 91c (1998); H. Appelshäuser et al. (NA49 Collaboration), Phys. Lett. B **459**, 679 (1999); J.G. Reid (NA49 Collaboration), Nucl. Phys. A **661**, 407c (1999)
9. M. Asakawa, U. Heinz, B. Müller, Phys. Rev. Lett. **85**, 2072 (2000)
10. S. Jeon, V. Koch, Phys. Rev. Lett. **85**, 2076 (2000)
11. T. Hatsuda, T. Kunihiro, Phys. Rep. **247**, 221 (1994); T. Kunihiro, Phys. Lett. B **271**, 395 (1991)
12. S. Gottlieb et al., Phys. Rev. Lett. **59**, 2247 (1987); Phys. Rev. D **38**, 2888 (1988); R. Gavai, J. Potvin, S. Sanielevici, Phys. Rev. D **40**, R2743 (1989)
13. M. Prakash, I. Zahed, Phys. Rev. Lett. **69**, 3282 (1992)
14. M. Prakash, R. Rapp, J. Wambach, I. Zahed, hep-ph/0110070
15. R. Gavai, S. Gupta, Phys. Rev. D **64**, 074506 (2001); R.V. Gavai, S. Gupta, P. Majumdar, hep-lat/0110032
16. H.B. Callen, T.A. Welton, Phys. Rev. **122**, 34 (1961); R. Kubo, J. Phys. Soc. Japan **12**, 570 (1957); D. Forster, Hydrodynamic fluctuation, broken symmetry and correlation functions (Benjamin/Cummings, Melno Park, CA 1975)
17. E. Braaten, R.D Pisarski, T.C Yuan, Phys. Rev. Lett. **64**, 2241 (1990)
18. J.I. Kapusta, Finite-temperature field theory (Cambridge University Press, Cambridge 1989)
19. M. Le Bellac, Thermal field theory (Cambridge University Press, Cambridge 1996)
20. J.-P. Blaizot, E. Iancu, R.R. Parwani, Phys. Rev. D **52**, 2543 (1995)
21. E. Braaten, T.C. Yuan, Phys. Rev. Lett. **66**, 2183 (1991)
22. F. Karsch, M.G. Mustafa, M.H. Thoma, Phys. Lett. B **497**, 249 (2001)
23. J. Frenkel, J.C. Taylor, Nucl. Phys. B **334**, 199 (1990)
24. J.O. Andersen, E. Braaten, M. Strickland, Phys. Rev. Lett. **83**, 2139 (1999)
25. S. Gupta, Phys. Rev. D **64**, 034507 (2001)
26. J.-P. Blaizot, E. Iancu, A. Rebhan, Phys. Rev. Lett. **83**, 2906 (1999)
27. J.-P. Blaizot, E. Iancu, A. Rebhan, hep-ph/0110369

Note added in proof: After completing our investigation a preprint by Blaizot, Iancu, and Rebhan appeared on the same topic [27]. They computed the quark number susceptibility from the thermodynamic potential, obtained in an approximately self-consistent resummation of HTLs. However, they do not use the effective HTL resummed vertices, which plays an important role by partly compensating the Landau damping contribution in the quark number susceptibility as shown in our investigation. As in the present paper, they found results similar to lattice data.